Approved For Release
2009/08/26 :
CIA-RDP88-00904R000100110

Third United Nations International Conference on the Peaceful Uses of Atomic Energy

A/CONF.28/P/362
USSR
May 1964
Original: RUSSIAN

Confidential until official release during Conference

NEUTRON PHYSICAL CHARACTERISTICS OF U+Be and U+BeO SYSTEMS

I.I.Bondarenko, V.P.Garin, R.K.Goncharov, E.S.Glushkov, O.A.Elovsky, I.I.Zaharkin, I.V.Istomin, V.G.Kosovsky, A.M.Krutov, V.A.Kuznetsov, V.I.Lependin, A.I.Leypunsky, S.S.Lomakin, I.G.Morozov, Uj.A.Nechaev, V.I.Nosov, N.A.Petushkova, N.N.Ponomarev-Stepnoy, S.P.Sazonov, O.N.Smirnov, I.E.Somov, E.A.Stumbur, L.A.Chernov, I.I.Shadura

INTRODUCTION

Beryllium and beryllium oxide due to their good moderating properties and additional neutron multiplication through the reaction $Be^9(n, 2n)$ can be used widely in reactor technology. Various U+Be, U+BeO systems have been studied in the USSR at the Kurchatov Atomic Energy Institute and at the Institute of Physics and Power.

In the paper basic results are given of works performed during last years.

I. STUDY OF U^{235} + Be INTERMEDIATE-NEUTRON SYSTEMS

A systematic study of critical parameters and physical characteristics of intermediate uranium-beryllium systems with reflector was performed in the stand ИФ -4 [1] . The

critical assemblies were characterized by the equal thicknesses of the reflectors of the same composition (a two-layer reflector with the inner beryllium layer; see Table 1), by the same porosity (an air volume fraction) of 11.5% and the aluminium core-volume fraction poor variation.

The critical assemblies forms were hexahedral prisms assembled from fuel packets filled with a fissionable material and a moderator. As rule, the realized critical parameters were not minimum for each of the assemblies due to their non-uniformities which are control rod channels, safety system rod channels, a core form deviation from regular, etc. To account for these non-uniformities the measurements of the separate core parts and reflector reactivity coefficients were made.

In Table 1 the data on the composition and dimensions of the core and reflectors are given as are critical parameters of some uranium-beryllium intermediate systems studied in the stand ИФ-4.

In Fig.1 the uranium-235 critical mass is presented as a function of the volume with account taken for the experimental corrections for the non-uniformities. The errors of the critical mass and volume determination with all the corrections were no more than 1.0%.

Particular emphasis have been placed upon the uranium elements self-shielding effect and its influence on critical parameters and neutron spectrum. In the critical assembly ИФ-4-10 ($\rho_{Be} / \rho_{U^5} = 106$) the fission density distribution over a uranium-235 plate thickness have been measured. The results of the measurements presented in Fig.2.indicate that the self-shielding factor given by the relation $F = \int_{\delta_0} f(\delta)\, d\delta \,/\, f(\delta_0)\,\delta_0$ is equal to 0.84. Here $f(\frac{\delta}{\delta_0})$ is the fission density distribution over the plate thickness, δ_0 is the uranium-235 plate thickness.

Nevertheless the critical masses of the assemblies ИФ-4-10, ИФ-4-14 and ИФ-4-15, which are with a different degree of their heterogeneity, were the same within the experimental errors. The results of these experiments support the conclusions of reference [1] which

experimentally shows (for an essentially more hard system with $\rho_{Be}/\rho_{U^5} = 31$) that in intermediate reactors, in spite of considerable self-shielding of fissions in thick uranium layers, the effect of 1 g of uranium-235 on reactivity is practically the same for all uranium layer thicknesses in samples (from $2.3 \cdot 10^{-2}$ g/cm^2 to 32 g/cm^2). From these data it can be concluded that the intermediate heterogeneous reactor critical parameters do not differ practically from the critical parameters of a proper physically homogeneous reactor. However, in the transition from a homogeneous to heterogeneous reactor neutron spectrum, naturally, becomes considerably softened. In Fig.3 the cadmium ratio for uranium-235 fissions number is given as a function of the thickness of uranium elements in the core cells of the assemblies ПФ-4-10, ПФ-4-14 and ПФ-4-15.

At the stand ПФ-4 the neutron spectra were measured in the energy range from 0.1 eV to ~50 eV with a mechanical neutron selector [2] with the variable rotor speed. The selector rotor with a 240 mm diameter was fabricated of getinux and furnished with a system of cruciformly located slits of a barrel-wise form. A spherical ion chamber with He^3 at pressure of 18 atm was used as a neutron detector. The beam shining surface was a square 5 by 5 cm. As an example in Fig.4 there are presented results of the measurements of neutron spectrum in the energy range from 0.1 eV to 50 eV performed in the critical assembly ПФ-4-12 ($\rho_{Be}/\rho_{U^5} = 209$). The measurements were made with the neutron impulse width of ~50 microseconds and with the flight length of 6 meters.

The beam shining surface was relatively at distances ~2 cm and ~22 cm from the reactor axis in the measurements of the spectrum in the central core region and in the peripheral core region (hexahedral core corner packet).

In processing of the experimental results corrections for detector effectiveness, for transmission function, for resolution and neutron flux gradient were introduced.

II. NEUTRON PHYSICAL CHARACTERISTICS OF U+Be, U+BeO THERMAL NEUTRON SYSTEMS

An experimental study of enriched uranium systems was performed in critical assemblies which were parallelepipeds

from moderator blocks and flat fuel elements, which were arranged in horizontal planes between the moderator blocks.

Caked beryllium oxide blocks and plates with size 100x100x50 mm, 50x50x50 mm, 100x50x15 mm and metallic beryllium plates with size 100x50x10 mm were used as moderators. The beryllium oxide density in these blocks was 2.8 g/cm^3, the beryllium plates density was 1.8 g/cm^3.

Fuel elements, which were made on base of teflon-4 with 90% enriched uranous-uranic oxide [3], contained an average of 1.775 g of uranous-uranic oxide and were with a square 100x100 mm and a thickness of 0.5 mm.

The effect of neutrons reflected from the walls and stand constructions was determined experimentally.

All the beryllium oxide moderated assemblies with a cell pitch of 5 cm had upper and bottom reflectors with a thickness of 2.5 cm. The beryllium moderated assemblies with a cell pitch of 0.5 cm had upper and bottom reflectors with a thickness of 0.5 cm. In the experiments the efficiency of the reflectors was found to be equal to their geometrical thickness with such reflector sizes.

The experimental data obtained on critical assemblies were used in calculations performed numerically by the multigroup method [4] on a digital computer and using the relation

$$K_{eff} = \frac{K_\infty \, e^{-B^2 \tau}}{1 + B^2 L^2} \qquad (1)$$

The critical assembly parameters and calculational results are presented in Table II.

Due to absorption in the reaction $Be^9(\gamma, n)$ of γ-rays from long-life fission products photoneutrons, which should be taken into account in the transient processes analysis, are producted apart from the delayed neutrons in systems containing beryllium.

Using the data on the delayed neutron and photoneutron yields reported in reference [5], the experiments consisted of measurements of reactivity, delayed neutron and photoneutron efficiencies were processed, calculations of the errors due to the asymptotic period measurements were performed.

The deviation of the measured positive period from asymptotic δ was determined for different times of reactor operation at constant power level. Calculational results are presented in Fig.5. For the beryllium oxide moderated assembly the deviation of the measured period from asymptotic was also determined experimentally (see, Fig.6).

For the beryllium oxide moderated assembly the quantity γ, which was assumed the same for all the groups of the delayed neutrons and photoneutrons, was determined by the method of replacement of fuel by an absorber.

In these experiments plates especially fabricated from teflon-4 with boron filling were used as absorbing elements. The experimental procedure consisted in the replacement of fuel elements by absorbing elements and in the reactivity measurement in mm of the control rod length.

It proved γ to be equal to 1.15 for the beryllium oxide moderated assembly studied; the experimental error was 4%.

The calculational γ value proved to be equal to 1.14.

In assemblies experiments were performed in which the critical assembly reactivity variation with a small change in the assembly dimensions was determined. Experimental data processing was conducted using the relation.

$$H = \left[2\pi^2 \left(\tau + L^2/1 + B^2L^2\right)\right]^{1/3} \left(\partial h/k_{eff}\,\partial\rho\right)^{1/3} \qquad (2)$$

where $H = h + \delta$, h is the core size, δ is the extrapolated addition or the effective thickness of a reflector in case of an assembly with a reflector.

Using the beryllium oxide and beryllium diffusion parameters reported in this paper the τ values were determined from these experiments and from the critical condition $K\infty$ was determined.

The data obtained are presented in Table III.

The neutron spatial distribution measurement was used to determine the neutron physical parameters and subcriticality degree of the systems studied.

In the case of a system, form of which is a rectangular parallelepiped, the ratio of the neutron flux in an assembly

with no uranium to the neutron flux in a subcritical assembly with uranium can be written as

$$f = \frac{\sum_{uvw} \left[S_{uvw} e^{-B^2_{uvw}\tau} / \Sigma_c^2 (1+B^2_{uvw} L_z^2) \right] \cos\frac{u\pi x}{a_э} \cos\frac{v\pi y}{b_э} \cos\frac{w\pi z}{c_э}}{\sum_{uvw} \frac{S_{uvw} e^{-B^2_{uvw}\tau}}{\Sigma_c (1+B^2_{uvw} L^2)(1-k_{uvw\,eff}} \cos\frac{u\pi x}{a_э} \cdot \cos\frac{v\pi y}{b_э} \cos\frac{w\pi z}{c_э}} \quad (3)$$

This relation, which can be considerably simplified if to neglect by the harmonics of order higher than third and to check such an experimental geometry that the third harmonic becomes zero, was used to determine the beryllium oxide moderated critical assembly subcriticality degree.

The neutron distribution was measured in experiments with indium foils.

The measured thermal neutron distribution in assemblies with no fissionable material and with a neutron source in the centre was used to determine the age value τ. For beryllium oxide τ of the Po + Be source neutrons proved to be equal to 128 ± 13 cm^2.

To study the neutron physical characteristics of a beryllium moderated assembly with two fuel elements in a layer the pulse-source method was also used. In the experiments a neutron generator of neutrons with energy of 14 MeV was applied. The damping constant dependence on the geometrical parameter was established from the experiment. The treatment of the dependence was performed by the least square method. The following parameters were obtained:

$$K_\infty = 2.23 \pm 0.05;\ L^2 = 20.7 \pm 1.5 \text{ cm}^2;$$
$$\alpha_\infty = (1.74 \pm 0.18) \cdot 10^{-4} \text{ cek}^{-1};$$
$$K_{Be} = 1.12 \pm 0.05;$$
$$\beta = (6.68 \pm 1.08) \cdot 10^{-3}.$$

III. STUDY OF U-Be LATTICES WITH NATURAL AND LOW ENRICHED URANIUM

The experiments were performed in a critical assembly which was a cylinder of metallic beryllium (mean density $\gamma = 1.75$ g/cm^3) with a diameter of 116 cm and a height of 100 cm, surrounded with an all-sided graphite reflector of 60 cm thickness. In the critical assembly core there were

362

89 vertical holes of 45 mm diameter located in chess-board order, which permitted to form lattices with pitches of 11.3 cm or 16.0cm. From the core centre a horizontal hole was extracted of 40 mm diameter for the measurement of the neutron spectrum over the cell.

As fuel natural and 2% enriched uranium blocks assembled in worker channels were used. The blocks were uniform in their dimensions and configuration and differed only in enrich ment and U^{235} content per block unit length.

The core dimensions permitted criticality to be achieved with 2% enriched fuel for both indicated pitches. To study the multiplication factors of natural uranium lattices two-region systems with the natural uranium central region were assembled . Criticality was achieved with the external region, which was assembled from 2% enriched channels. In Table IV the critical dimensions are given for 2% enriched fuel.

For four lattices tnere were measured the infinite neutron multiplication factors k_∞ and the thermal neutron spectra over the cell.

The experimental measurement of k_∞ and its cofactors was based on a method reported in reference [6] with rather modified measurement technique and results processing procedure.

Accordingly to [6]

$$K_\infty = \mu\varphi\theta\nu_{eff} = \frac{\nu_5^f + (\nu_8^f - 1)\,\Pi_8^f/\Pi_5^f}{\Pi_5/\Pi_5^f + \Pi_3/\Pi_5^f + \Pi_8^\tau/\Pi_5^f} \qquad (7)$$

$$\mu = 1 + \frac{(\nu_8^f - 1)\,\Pi_8^f/\Pi_5^f}{\nu_5^f} \qquad (8)$$

$$1 - \varphi = \frac{(\Pi_8^R/\Pi_5^f)}{\Pi_5/\Pi_5^f + \Pi_3/\Pi_5^f + \Pi_8^\tau/\Pi_5^f} \qquad (9)$$

$$1 - \theta = \frac{\Pi_2 \ell \Pi_5^f}{\Pi_5/\Pi_5^f + \Pi_3/\Pi_5^f + \Pi_8^{1/v}/\Pi_5^f} \qquad (10)$$

$$\nu_{eff} = \frac{\nu_5^f}{\Pi_5/\Pi_5^f + \Pi_8^{1/v}/\Pi_5^f} \qquad (11)$$

where:

Π_5^f and Π_8^f - number of fission neutron absorptions in uranium-235 and uranium-238 relatively;

362

Π_5 - total number of neutron absorptions in uranium-235;

Π_8^r, Π_8^K, $\Pi_8^{1/v}$ - relatively total number of neutron radiative absorptions, number of radiative absorptions in the resonance region and number of radiative absorptions due to $\frac{1}{v}$ cross-section in uranium-238 ($\Pi_8^r = \Pi_8^K + \Pi_8^{1/v}$);

Π_3' - number of neutron absorptions in moderator and structural materials.

The number of neutron absorptions in lattice components was determined from measurement of relavitve activities of detectors, which were exposed in the central cell of studied lattices. The detectors were 35 mm - diameter foils of uranium-235 (90% enriched), depleted uranium ($3 \cdot 10^{-3}$% of uranium-235), natural uranium, thorium, vanadium and copper.

A packet of several detectors, thin (1.5 mm) uranium washers of a lattice studied and protective aluminium foils was assembled in a special experimental channel (Fig.7) and was placed in the central cell for exposure.

The absorptions number in beryllium (Π_3) was determined from the measurements of the neutron density distribution over the cell (Fig.8) with copper and vanadium detectors. Exposure of all the detectors was performed both with no cadmium and with cadmium jackets. The correction for "eating away" of the resonance and fast neutron flux due to cadmium was determined experimentally.

The detectors activity measurement was performed with a scintillation counter and a 128-channel amplitude analyzer. All the measurements of the absorptions in lattice components were made relatively to the number of fission neutron absorptions in uranium-235 (Π_5^f).

Using the experimental data and formulae (4+8) K_∞, μ, φ, θ, V_{eff} and P (breading coefficient) were calculated of the lattices studied. The calculational results are given in Table V.

362

In the multiplication parameters calculations the following constants values were assumed

$$\nu_5^f = 2.43 \pm 0.02$$
$$\nu_8^f = 2.9 \pm 0.1$$
$$\sigma_5^f = (582 \pm 4).10^{-24} \text{ cm}^2$$
$$\sigma_8^c = (2.75 \pm 0.04).10^{24} \text{ cm}^2$$

By Urtseva V.I. the parameters experimentally determined as functions of a lattice pitch have been calculated in the two-group diffusion approximation. For comparison the calculational and experimental K_∞ values are presented in Fig.9.

In the uranium-beryllium systems study the thermal neutron spectra were also measured in several 2% enriched and natural uranium lattices with a mechanical monochromator [9] .

The thermal neturon spectra obtained on a cell boundary for two lattices are given in Fig.10 . The experimental points were processed by the method of least squares with a crude description of the spectrum near its maximum as the maxwellian distribution. It is appeared that only the spectrum over the maximum can be fitted to the maxwellian distribution that conforms to the calculations by Nelkin and Cohen [10] .

To compare the experimental data with the theoretical results by Smelov V.V. and Ilyasova G.A. the 15-group calculation have been made of the thermal neutron space-energy distribution over the cells studied in a P_3 - approximation using a model to account for the crystal bindings in the thermalization region.

IV. STUDY OF BERYLLUM REFLECTOR EFFECT IN FAST NEUTRON REACTOR

A decreasing of beryllium fraction and an increasing of fuel enrichment in the reactor core leads to the neutron spectrum hardening.

As a limiting case, in this sense, a reactor can be considered in which the core contains only fuel of maximum

enrichment, and moderator (beryllium) is present only in a reflector.

Such a system can be identified as a "fast reactor with a moderating reflector" x).

In w958-1961 two physical beryllium reflected fast reactors, БР-4 and БР-6, were studied. The reactor shapes were right hexagonal prisms. The cores were assembled from almost-close-packed rod-type fuel elements (plutonium elements in БР-4 and 90% enriched uranium elements in БР-6).

The beryllium reflectors can be replaced in the thickness range from 4 cm to 15 cm.

For beryllium reflector thickness more than 5-6 cm the spatial distributions of the main reaction ($U^{235}(n,f)$ in БР-6 and Pu^{239} (n,f) in БР-4) density differ essentially from the distributions in common fast reactors with non-moderating reflectors.

For this fission density flattening occurs over the core radius due to intermediate energy neutrons penetrating out of a reflector.

Near the core boundary a sharp fission density jump forms, for the most part, due to subcadmium energy neutrons. Whereas the U^{238} fission density behaviour is practically independent upon the reflector thickness with asymptotic character held (see, Fig.11).

The main isotope fission density jump on the core boundary (a difference between the true and asymptotic fission densities) increases with the increased reflector thickness.

With the reflector thickness $\Delta = 5 \div 6$ cm the jump disappears, i.e., a more thin beryllium reflector does not already make cardinal changes in the fission density distribution.

The central core part for all the БР-4 and БР-6 variants maintained a hard neutron spectrum. The typical $\sigma_f(U^{235})/\sigma_f(U^{238})$ value was ~7 and ~9 in the БР-4 centre and in the БР-6 centre respectively.

---

x) Similar fast-thermal systems have been studied until recently by a number of authors [11, 12, 13].

Intergrating of the fission density over the core indicated that the fission fraction due to neutrons with energies $E > 1.4$ Mev was 20-30% (with the reflector thickness of 8-12 cm). The thermal-neutron fission fraction was estimated from change of K_{eff} due to a cadmium shield inserted between the core and the reflector. It equals 1 + 2% with the reflector thickness of 8-10 cm and 4+ 5% with the thickness of 12-15 cm.

The thickness of the reflector varying, its albedo and spectrum of neutrons returned by it change.

The slowing-down neutrons spectra in thin reflectors can not be considered as the pure Fermi spectrum, because there is a large neutron leakage in slowing-down. The slowing-down neutrons spectrum form can be obtained similar to the slowing-down spectrum in an infinite medium with the energy-independent cross-section Σa, i.e., of the $1/E^m$ form (see, [15]).

The Σa role in this case is played by $\frac{\lambda_{tr} B^2}{3}$ where B^2 is the geometrical parameter of a reflector with the thickness Δ.

In the age model $m = 1 - \lambda_{tr} \lambda_s B^2/3$ $\xi = f(\Delta)$

When the reflector thickness decreases from 15 cm to 8 cm, the value of m decreases from 0.9 to 0.7. With the reflector thickness $\Delta < 4$ cm value of $m < 0$, i.e. the flux spectrum does not increase with decreasing of energy, but decreases that is typical for fast reactors. Interpretation carried out shows that a limit thickness $\Delta \sim 4$ cm ($m = 0$) exists which as if separates the common fast reactors from the class of the "fast reactors with a moderating reflector". The $1/E^m$ spectrum form was confirmed by S.A.Katishev's measurements of the resonance detectors activation in reflectors.

In Fig.12 the results of the measurements, the straight line which corresponds to $1/E^m$, and also the spectrum hystogram obtained from the multigroup calculation[x)] are shown, The simulation of the spectrum in a moderating reflector with account taken for a possible distinction from the Fermi

---

x) The calculations were performed by E.I.Lyashenko under the guidance of G.I.Marchuk.

spectrum permits, for example, to eliminate the discrepancy of the experimental and calculational R_{cd} values reported in reference [II].

In the thin reflectors considered the incomplete neutron thermalization effect becomes also apparent which results in the anomalously high ratio of the subcadmium $\sigma_f(Pu^{239})/\sigma_{n\alpha}(B^{10})$.

The prompt neutron mean life time "l" in the systems considered is essentially less than in thermal reactors, but more than in fast reactors

The measurements made by the Rossi-α and boron poisoning methods[x] (with $\beta_{eff} = 0.007$) gave for the reactor БР-6 the values which increase with the increased reflector thickness: with $\Delta = 8$ cm; $l = 10^{-6}$ sec; with $\Delta = 12$ cm; $l = 5.10^{-6}$ sec.

The performed measurements of disturbances allowed to verify an applicability to moderating reflectored fast reactors of the "degree law" which characterizes through the exponent n(x) the effect of the each diluent "x" on critical mass (see, [I4]). The measurements shows that the values n(x) decrease with the increased reflector thickness and can even be negative.

In БР-6 with $\Delta = 10$ cm: n(void) = 1.44 ; $n(U^{238}) = 0.95$; $n(Be) = 0.84$ and $n(H_2O) = 0.30$. And with $\Delta = 14$ cm: n(void) =0.83; $n(U^{238}) = 0.44$; $n(Be) = 0.29$; $n(H_2O) = -0.20$

REFERENCES

I. А.И.Леипунский и др. "Экспериментальные исследования некоторых физических особенностеи промежуточных реакторов с бериллиевым замедлителем Proceedings of the Conference on Fast and Intermediate Reactors Physics. Vienna, 1962.

2. В.А.Кузнецов и др."Гидриды металлов как замедлители неитронов в реакторах". Proceedings of the Conference on Fast and Intermediate Reactors Physics. Vienna, 1962.

3. Н.Н. Пономарев-Степной, С.С. Ломакин, Ю.Г. Дегальцев, Атомная энергия, 15, 259 (1963).

4. Г.И.Марчук. "Методы расчета ядерных реакторов". Атомиздат, Москва, 1961.

5. G.R.Keepin, Nucleonics, 20 (1962) 151.

x) The measurements were performed by D.M.Shvetsov and V.H. Manohin.

362

6. С.М.Фейнберг и др. Выгорание горючего в водо-водяных энергетических реакторах и эксперименты с уран-водной решеткой.
Proceedings of the Second International Conference on the Peaceful Uses of Atomic Energy, Geneva, 2I45 (1958)

7. А.К.Красин и др. Изучение физических характеристик реактора с бериллиевым замедлителем.
Proceedings of the Second International Conference on the Peaceful Uses of Atomic Energy, Geneva, 2I46 (I958)

8. И.Ф.Жежерун, И.П.Садиков, В.А.Гарабанько, А.А.Чернышев. Атомная энергия", I5, 485 (I962).

9. А.П.Сенченков, Ф.М.Кузнецов. "Атомная энергия", 5, I24 (I958)

IO. М.С.Нелкин, Е.Р.Коуэн. "Нейтронная физика" (сборник), 654, М. Атомиздат, I959.

II. R.D.Smith and J.E. Sanders "Experimental Work with Zero Energy Fast Reactors". Proceedings of the Second Conference on the Peaceful Uses of Atomic Energy, Geneva, 39 (I958)

I2. R.Avery et al. "Coupled Fast-thermal Power Breeder Critical Experiment. Proceedings of the Second International Conference on the Peaceful Uses of Atomic Energy, Geneva, 2I60 (I958)

I3. H.H.Hummel et al. "Experimental and Theoretical Studies of the Coupled Fast-Thermal System ZPR-V". Proceedings of the Second International Conference on the Peaceful Uses of Atomic Energy, Geneva, 599 (I958).

I4. G.E.Hansen et al. Nucl.Sci. and Engng. 8, 543 (I960)

I5. Weinberg A., Wigner E. The Physical Theory of Neutron Chain Reactors. University of Chicago Press, I958.

Table I

Critical Parameters of the ПФ-4 Assemblies

Assembly	Nuclear concentrations ratio $\rho_{Be}/\rho_{U^{235}}$	Beryllium thickness in a cell (cm)	Uranium-235 thickness in a cell (cm)	Effective Be-reflector thickness (cm)	Effective Fe-reflector thickness (cm)	U-235 critical mass (kg)	Volume beryllium content in a core ε Be %	Volume enriched uranium content in a core ε_u (%)	Volume aluminium content in a core ε Al (%)	Core height (cm)	Equivalent core diameter (cm)	Critical volume (10^3 cm^3)	Volume nickel content ε Ni (%)
ПФ-4-09	0	0	0	13.9	9.2	20.81	0	64.4	24.0	12.7	13.9	1.93	-
ПФ-4-07	1.76	0.5	0.5	13.9	13.9	25.22	27	42.7	19.7	23.2	13.9	3.53	-
ПФ-4-13	12.8	0.5	0.12	13.9	9.2	25.29	59.2	13.5	14.7	26.4	23.3	11.22	1.0
-		64% 2.0 (36%)											
ПФ-4-08	53.6	0.5	0.03	13.9	13.9	18.15	70.2	4.0	13.9	28.9	31.3	28.34	0.4
ПФ-4-10	106	1.0	0.03	13.9	9.2	14.26	72.4	2.0	13.9	31.2	41.8	42.76	0.2
ПФ-4-11	157.9	1.5	0.03	13.9	9.2	11.84	73.1	1.3	13.9	39.2	41.8	53.69	0.15
ПФ-4-12	209	2.0	0.03	13.9	9.2	10.14	73.5	0.9	13.9	43.0	41.8	58.89	0.10
ПФ-4-14	106	2.0	0.06	13.9	9.2	14.15	72.4	2.0	13.9	30.9	41.80	42.41	0.2
ПФ-4-15	106	3.0	0.09	13.9	9.2	14.62	72.4	2.0	13.9	32.0	41.8	43.83	0.2

Table II

Beryllium oxide and beryllium moderated critical assemblies

Moderator	Number of fuel elements in a layer	U-235 mass [g]	Cell pitch [cm]	Atomic ratio BeO/U-235	$B^2 \cdot 10^2$ [cm^{-2}]	K_{eff} calculation using experimental parameters	K_{eff} multigroup calculations
Beryllium	1	2803	5	8699	0.274±0.005	1.04041 x)	1.01623
	2	3060	5	4904	0.376±0.005	1.01423	0.99028
	3	3409	5	3272	0.438±0.005	0.99872	0.96684
	4	4225	5	2464	0.478±0.005	0.99178	0.96739
	5	4828	5	1974	0.488±0.005	0.98878	0.97191
	4	3528	10	4907	0.357±0.005	1.00642	0.98028
	6	4232	10	3262	0.414±0.005	0.98474	0.97070
	8	5146	10	2464	0.455±0.005	0.96606	0.96468
	10	5749	10	1965	0.463±0.005	0.96977	0.97808
Beryllium	1	3292	1	3481	0.654±0.008	0.99002	0.98206
	2	5790	1	1745	0.677±0.008	0.99785	0.98537
	3	8344	1	1165	0.666±0.008	0.99574	0.98578

x) An assembly with non-uniform fuel distribution which was not taken into account in the calculations.

Table III

Experimental data for assemblies from beryllium oxide and beryllium

Moderator	Number of fuel elements in a layer	K_∞	τ [cm^2]
Beryllium	1	2.24 ± 0.06	97.1 ± 3.1
Beryllium	2	2.28 ± 0.06	104.6 ± 1.2
Beryllium oxide	3	2.07 ± 0.06	112.0 ± 2.5

Table IV

Critical charges and critical sizes for 2% enricned fuel

Lattice pitch [cm]	Core height [cm]	Core radius [cm]	U-235 charge [kg]
16.0	100	60.5	4.50
11.3	100	37.2	3.40

362

Table V

Multiplication parameters in uranium-beryllium systems

Parameter	Natural uranium		2 % enriched uranium	
	a pitch of 11.3 cm	a pitch of 16.0 cm	a pitch of 11.3 cm	a pitch of 16.0 cm
μ	1.06 ± 0.01	1.06 ± 0.01	1.020±0.003	1.017±0.003
ν_{eff}	1.31 ± 0.06	1.31 ± 0.05	1.69 ±0.05	1.71 ±0.05
φ	0.76 ± 0.03	0.86 ± 0.03	0.89 ± 0.01	0.93 ±0.01
θ	0.92 ± 0.01	0.86 ± 0.01	0.89 ± 0.01	0.81 ±0.01
p	1.05 ± 0.03	0.85 ± 0.02	0.36 ± 0.01	0.30 ±0.01
K_∞	0.98 ± 0.03	1.02 ± 0.3	1.36 ± 0.04	1.31 ± 0.04
K_∞^{calc}	0.97	1.015	1.36	1.32
K_∞ / K_{Be}	1.08	1.12	1.50	1.44

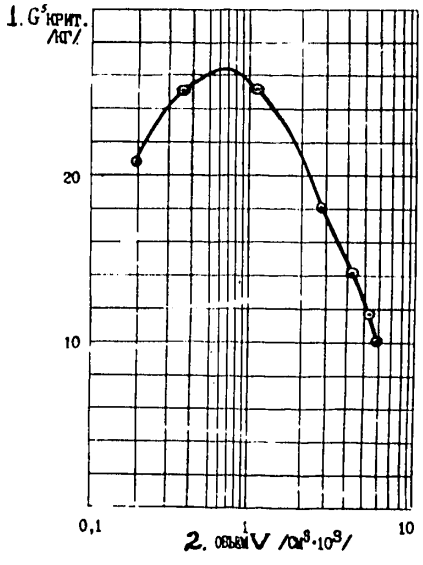

Fig. 1

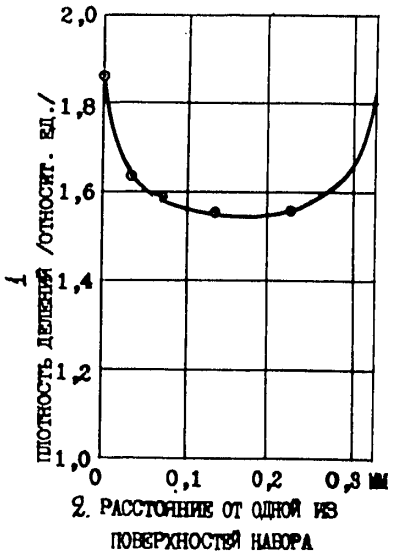

Fig. 2

Fig.1. The U-235 critical mass as a function of the critical volume.
1 - G^5 crit/kg/. 2 - volume V ($cm^3 \cdot 10^3$).

Fig.2. The fission density distribution over the thickness of a 0.33 mm U-235 layer.
1 - density fission (relative un.); 2 - distance from the surface of set.

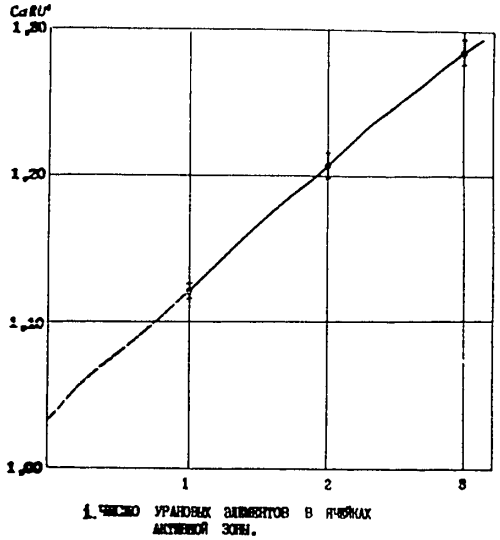

Fig. 3

Fig.3. The cadmium ratio as a function of the number of uranium elements in core cells with the homogenized ratio $\rho_{Be} / \rho_{U^5} = 106$.
1 - number of uranium elements in the core.

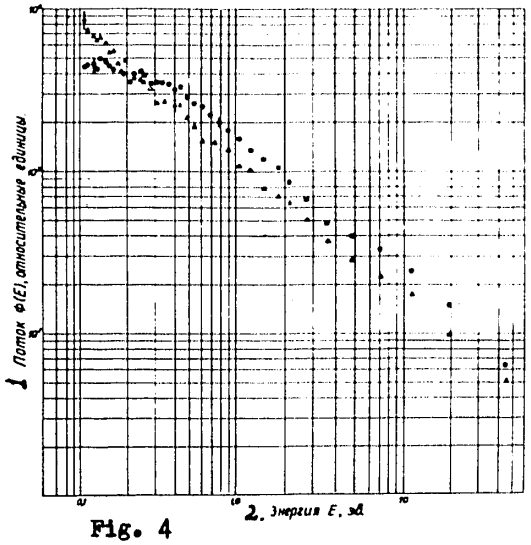

Fig. 4

Fig.4. The neutron flux energy distribution in the ПФ –4 assembly measured in the central and peripheral regions. The curves are normalized to power.
o - measurements in the central region measurements
▲ - measurements on the beryllium reflector boundary.
1 - flow Φ (E), relative unity;2 - energy E, eV.

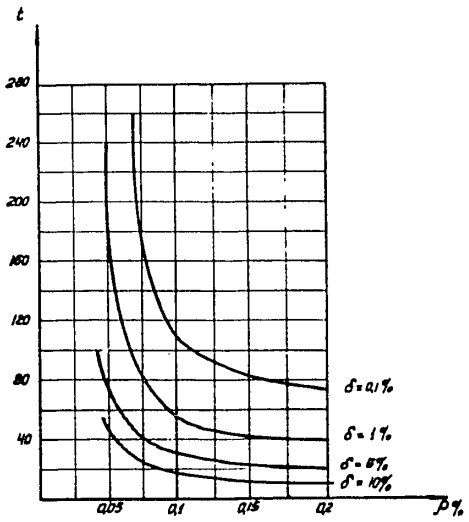

Fig. 5

Fig.5. The wait time before the period measurement following the reactivity jump as function of the reactivity value for various δ .
A(a) beryllium moderated critical assembly,
T = 1000 sec.
$\rho = 0.1.10^{-2}$, $l = 10^{-4}$ sec.
t - time following the reactivity jump, sec.
ρ - reactivity in per cents.

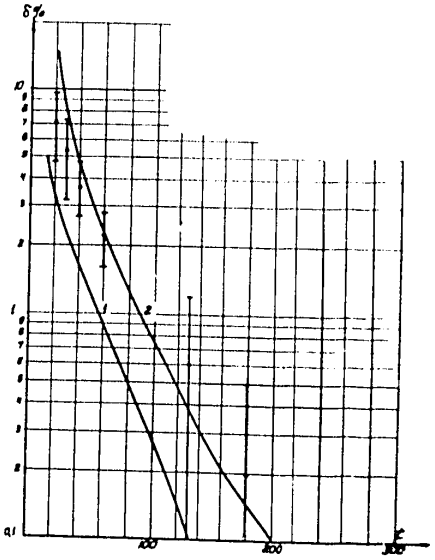

Fig.6. The deviation of the measured period from the asymptotic period as a function of time following the reactivity jump.
A(a) beryllium oxide moderated critical assembly,
T = 1000 sec, $\rho = 0.1 \cdot 10^{-2}$, $l = 10^{-4}$ sec.
1 - calculation with no account for photoneutrons ;
2 - calculation with photoneutrons taken into account.

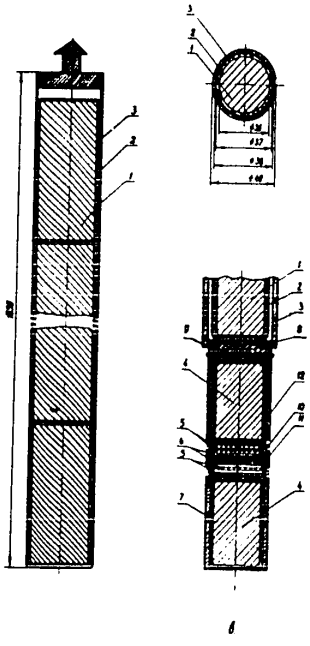

Fig.7.
Design of a work fuel element (a) and an experimental block (b).
1 - uranium blocks; 2 - Al block can; 3 - aluminium work channel tube; 4 - upper and lower parts of an experimental uranium block; 5 - uranium washer of a 1.5 mm thickness; 6 - protective foil of a 0.03 mm thickness; 7 - Al container; 8 - Al plug of the experimental channel upper half; 9 - fastener to attach the experimental block upper part to the experimental channel upper part; 10 - detector to be exposed; 11 - cadmium sneath; 12 - aluminium ring

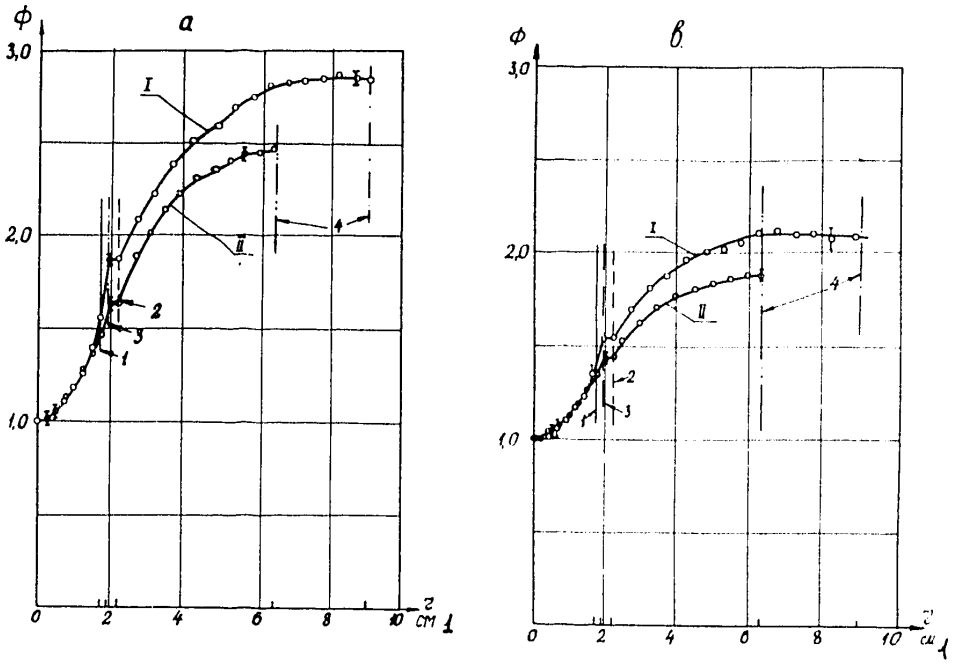

Fig.8. The thermal neutron density distribution over a cell:
a and b - 2% enriched uranium lattices with a pitch of 11.3 cm and 16,0 cm relatively;
c and d - natural uranium lattices with a pitch of 11.3 cm and 16.0 cm relatively;
1 - uranium boundary; 2 - Be moderator boundary;
3 - Al block can boundary; 4 - equivalent cell bounndary (1 - cm).

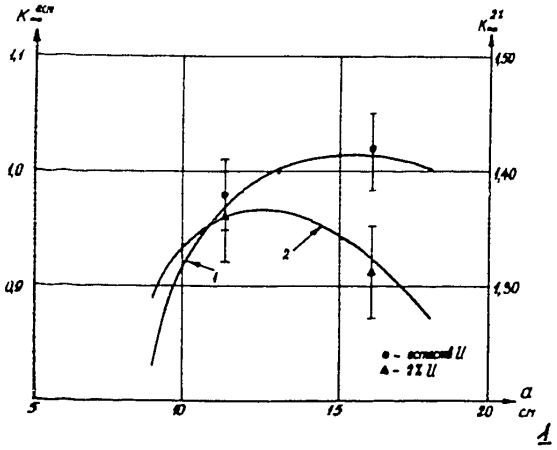

Fig.9. The uranium-beryllium lattice multiplication coefficient as a function of the lattice pitch:
1 - calculational curve for natural uranium;
2 - calculational curve for 2% enriched uranium .
(1 - natural U)

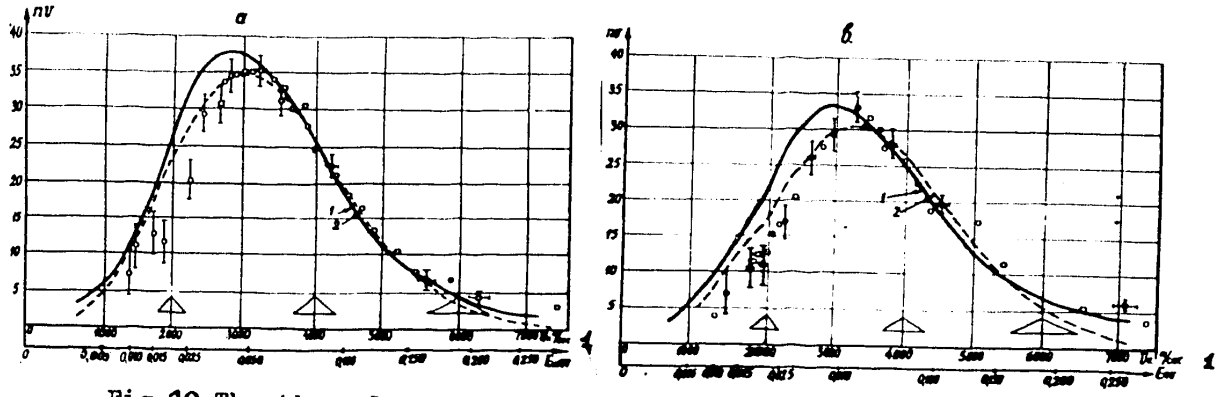

Fig.10. The thermal neutron flux spectra on the cell boundary (1 - cm).

a - 2% enriched uranium lattice (of a 16.0 cm pitch);

b - natural uranium lattice (of a 11.3 cm pitch).

1 - calculational spectrum for the model with account taken for the crystal effects; 2 - neutron flux maxwellian distribution curve.

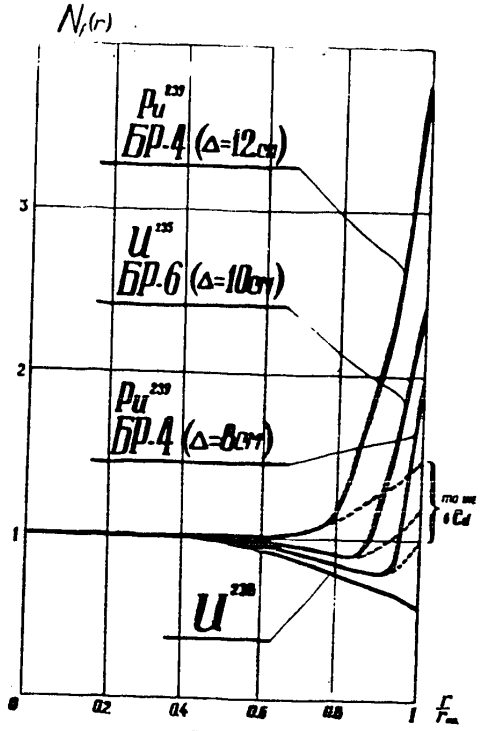

Fig. 11.

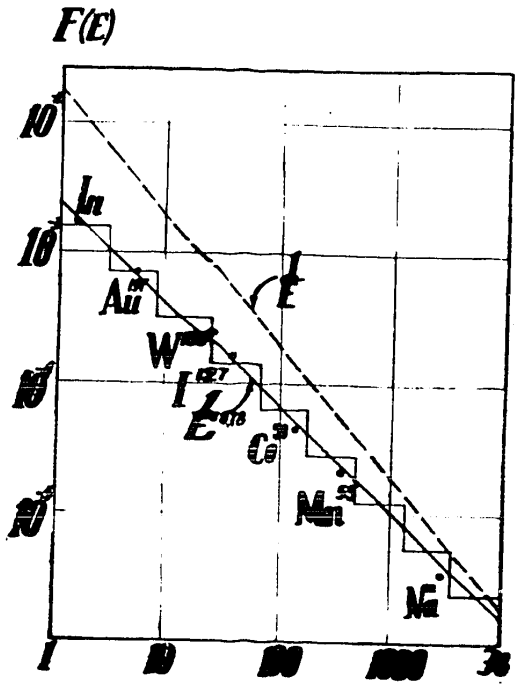

Fig. 12

Fig.11. The relative fission density distribution over the cell radius (Δ is the reflector thickness in cm)

Fig.12. The fission density jump "C" on the core boundary as a function of the reflector thickness.

(1-m/sec)

362

Third United Nations International Conference on the Peaceful Uses of Atomic Energy

A/CONF.28/P/362a
USSR
May 1964
Original: RUSSIAN

Confidential until official release during Conference

STUDY OF BERYLLIUM AND BERYLLIA AS NEUTRON MODERATORS

I.F.Zhezherun, A.K.Krasin, G.I.Plindov, I.P.Sadikov, V.A.Tarabanko, A.A.Chernyshgv

Introduction

Beryllium and beryllia are of interest in the nuclear engineering as construction materials of reactors of various types due to their good moderative properties, weak thermal neutron absorption and fast neutron multiplication in the reaction $Be^9(n,2n)$. Physical properties of beryllium and beryllia determining diffusion, moderation, scattering and multiplication of neutrons have been studied for a few years in the Kurchatov Institute of Atomic Energy (IAE). The main results are briefly presented in the report.

In addition, the fast neutron multiplication data obtained from the analysis of the critical assemblies in the Institute of Energetics of Academy of Science BSSR are presented.

A. STUDY OF BERYLLIUM AND BERYLLIA AS NEUTRON MODERATORS (1)

I.F.Zhezherun, I.P.Sadikov, V.A.Tarabanko, A.A.Chernyshev
(The Kurchatov Institute of Atomic Energy)

1. Effect of beryllia microstructure and temperature on thermal neutron scattering cross-section

The microcrystallyne structure can essentially influence on the moderative and scattering properties of beryllia due to the effect of size and orientation of crystal grains on the scattering cross-section σ_s. It is known that with the increasing of the grain size σ_s decreases due to the extinction effect; their advantageous orientation (texture) which can appear in pressing or pressing out of BeO articles can cause the anisotropy of σ_s. To make clear how much these effects are to be taken into account when calculating the reactors of BeO moderator, the total cross-section σ_t ($\sigma_t \simeq \sigma_s$ for BeO) was measured with the chopper for four samples with various grain size (see Fig.1). Sample 1 consisted of the plates 1.2x7x21 mm produced by pressing out, sample 2 of the rods 3x4x23 mm produced by pressing, sample 3 made of the discs 30 mm in diameter, 3 mm thick produced by pressing out and sample 4 of the discs 38 mm in diameter, 3 mm thick produced by cold pressing. The microstructure analysis of the samples, carried out by Yu.G.Digaltsev and V.I.Kushakov, showed the all samples are closed packed crystallite of irregular polyhedron form. The grain sizes are shown in Fig.1, the mean size was determined as a square root of an average area of a grain in a microsection photograph. In different measurements the sample thickness varied between 3.2 g/cm^2 and 5.6 g/cm^2.

Under given experimental conditions the energy resolution was between 4 and 10% in the range 0.03-0.1 ev. To observe the anosotropy of σ_t two series of measurements have been done with samples 1 and 2, the neutron beam being fallen both in parallel and normally to the directions of pressing or pressing out (Fig.2).

It is seen from these figures that at small energy (0.005-0.2 ev) the difference in σ_t is 40% for the samples with the grain sizes 8μ and 29μ ; it may cause 10%-change of the average spectrum scattering length λ_s or the square diffusion length L^2 (see Table 1). The extinction effect does not practically influence on σ_t if the grain size $\leq$ 10μ.

The presence of texture in the hexagonal BeO lattice seems to be observed in the best way from neutron wave reflection on the planes being normal or parallel to the c-axis of the crys-

tal elementary cell, i.e. from the reflections in which the first two indexes or the last one are equal to zero. The anisotropy of σ_t is observed from the reflection on the plane (110) at E = 0.012 ev (see inserts on Fig.2) as reaching 25% of the partial or 7% of the measured cross-sections. The values of the cross-sections $\sigma_{\perp}^{110}$ and $\sigma_{\parallel}^{110}$ show the advantageous orientation of the crystal grains by c-axis of the elementary cell in direction of pressing out and normally to the pressing direction, if the neutron beam is normal or parallel to the pressing out or pressing directions. For other reflections the difference in $\sigma_{\perp}$ and $\sigma_{\parallel}$, if it is, does not exceed the measurement errors. Thus, the anisotropy of σ_t is small and its influence on L^2 may be neglected.

In the range 1-10 ev where atom binding in the crystal lattice does not effect on scattering the measured value of σ_t is constant and equals 10 ± 0.15 barn for all the samples.

The temperature dependence of σ_t is of importance for the calculation of the temperature reactivity coefficient. In Fig.3 the measurement results of σ_t are shown for the sample of advantageous grain sizes 10-20μ at T = 290; 800; 1300; 1500°K. In Fig.4 the temperature dependence of $\sigma_t(E)$ for some energies is plotted as well as that of $\bar{\sigma}_t$ and $(\overline{\sigma_t^{-1}})^{-1}$ averaged over the Maxwellian spectrum (at the neutron temperature $T_H = T + 100°K$) and obtained from Fig.3.

The measured results reveal that with the sample heating: 1) the position of Bragg maxima are shifted towards less energies in accordance with the temperature expansion; 2) the value of the maxima decreases; 3) the value of $\bar{\sigma}_t$ increases, the greater it will be the less the neutron energy E is. At $E > 0.15$ ev $\bar{\sigma}_t$, $\bar{\sigma}_t$ and $(\overline{\sigma_t^{-1}})^{-1}$ have a minimum near T = 1300°K which can be explained by the competition of two processes: decreasing of the coherent elastic scattering and increasing of the coherent inelastic one with the temperature increase. Since oxygen and beryllium in BeO are anisotropic and the incoherent scattering in Be depending on the spin is small, the measured σ_t can be practically divided only in two terms: the elastic and inelastic coherent scattering cross-section, $\bar{\sigma}_t$ is mainly due to the latter at $E < 0.0035$ ev.

The change of σ_t with the temperature in the range 290-1500°K can lead to the decreasing of L^2 by about 20%.

The sample density was 2.80-2.85 g/cm^3, i.e. it was less than the theoretical value 3.04 g/cm^3. Therefore the question appeared whether the scattering in small angles, caused by the refraction and the diffraction of the neutron waves at the boundaries between substance and air in the sample pores, effects on the measured σ_t. The additional measurements on BeO sample in the form of the fine-grained dust showed that the scattering in small angles can be neglected.

2. Study of thermal neutron diffusion in beryllium and beryllia

The diffusion parameters of Be and BeO were studied by means of the pulse method with the linear accelerator of IAE. The method, as is known, is to measure the dampling coefficient α of the neutron density in the moderator block with time and to analyse consequently the dependence of α upon the block geometry parameter B^2:

$$\alpha = \Sigma_c v + DB^2 - cB^4 \qquad (I)$$

where $\Sigma_c v$ is the absorption velocity, D and C are the coefficients of diffusion and diffusion cooling respectively.

The coefficient α was measured for 30 beryllium blocks at $B^2 = 0.005$-0.11 cm^{-2} and for 27 beryllia blocks at $B^2 = 0.004$-0.095 cm^{-2} (see Fig.5). The average Be density in blocks was 1.79 g/cm^3, that of BeO - 2.79 g/cm^3. The measurements of α for such great number of the blocks allowed to obtain the more accurate diffusion parameters (see Table II) than these in [2-8].

The all experimental values of the coefficient D for Be, including the ones in Table II, coincide within the measurement errors; for BeO the difference is considerably higher than the error. For the coefficient C the data are in agreement for BeO but as for Be there is

no such agreement,

The study of the cause of the experimental data dispersion for D and C showed that it may be essentially connected with the possible difference of the crystal structure of the materials under investigation. Thus the estimated calculations of D and C for BeO using the above ϕ_t for the samples with the grain sizes 8 μ and 29 μ give the values of D within 10% and the values of C within 60%. The effect of the term with B^2 in Eq. I is negligible as it is seen from the additional analysis of measurements by means of the computer.

In [9] for the explanation of the dispersion of C it was indicated on the neutron trap effect which must result in dependence of α upon the measurement conditions for small blocks (the neutron source power, the background level etc.). Our attempts to detect this dependence for the Be block of 20 cm^3 when the source power changes 10 times and the background level does 5 times failed (Fig.6).

The value of C measured give some information on the neutron slowing-down near the thermal equilibrium indicating the decrease of the mean logarithmic energy loss ξ in Be and BeO approximately 4-5 times.

3. Measurement of moderation length in Be up to 1.46 ev and 0.3 ev

The slowing-down density $q(r,E_\tau)$ was measured in the rectangular prism 80x90x145 cm. The U^{235} converter, irradiated by the neutron beam of the reactor thermal column, served as a neutron source; the indium foils in cadmium filters were used as the neutron detectors at 1.46 ev; the small plutonium chamber in the filter with mixture of samarium and gadolinium oxides [10] was the detector at energy 0.3 ev. The measurement results are presented in Fig.7 (for In) and in Fig.8 (for Pu chamber).

The measurements by means of the Pu chamber were carried out in each point under the following conditions:

1) the chamber was surrounded by the filter of 0.125 g/cm^2 Sm and 0.04 g/cm^2 Gd (N_{SmGd});
2) the chamber was surrounded by the filter of 0.125 g/cm^2 Sm, 0.04 g/cm^2 Gd and 0.35 g/cm^2 Cd (N_{SmGdCd});
3) the chamber without filters (N).

The neutron flux of 0.3 ev was obtained as the difference of the first two measurements $\phi_{0.3} = N_{SmGd} - N_{SmGdCd}$, and the thermal neutron flux $\varphi_T = N - (1-T)^{-1} N_{SmGd}$, where T is the transmission of the resonance neutrons by the filter Sm+Gd. The inaccuracy of the value T, determined from the calculation, effects slightly on φ_T, since $N_{SmGd} \ll N$.

The curves for $\varphi_{0.3}$ and φ_T (Fig.11) at distances $\tau > 60$ cm from the source are parallel. It implies that at such distances the density of the slowing-down neutrons of 0.3 ev is negligibly small in comparison with the density of neutrons of the same energy in the established Maxwellian spectrum. Using the ratio $\varphi_{0.3}/\varphi_T = (6.58 \pm 0.1)\cdot 10^{-3}$ at distances $\tau > 60$ cm one can obtain the slowing-down density $q_{0.3}$ from the total flux $\varphi_{0.3}$.

From Figs.7, 8 it is seen that at distances $\tau \leq 30$ cm from the source the slowing-down density is approximated by the expression $q(\tau) \sim e^{-\tau^2/4\tau}$ with $\tau = 80 \pm 2$ cm^2 at $E_\tau = 1.46$ ev and with $\tau = 91.5 \pm 2.5$ cm^2 at $E_\tau = 0.3$ ev. At $\tau > 30$ cm the expression $q(\tau) \sim \tau^{-2} e^{-\tau/\lambda}$ is valid with $\lambda = 7.27 \pm 0.10$ cm at $E_\tau = 1.46$ ev and 0.3 ev; this expression presents evidently the density of the first collisions. Over the whole region of measurements ($\tau \leq 90$ cm) the kernel of moderation is well approximated by the expression (Fig.9)

$$K(\tau, E_\tau) = \sum_{i=1}^{3} \frac{P_i(E_\tau)}{(4\pi\tau_i)^{3/2}} e^{-\tau^2/4\tau_i} \qquad (2)$$

where $\tau_1 = 68 cm^2$, $\tau_2 = 130 cm^2$, $\tau_3 = 265 cm^2$

$P_1 = 0.0666$, $P_2 = 0.307$, $P_3 = 0.027$ at $E_\tau = 1.46$ ev

$P_1 = 0.541$, $P_2 = 0.422$, $P_3 = 0.037$ at $E_\tau = 0.3$ ev.

The square of moderation length (1/6 of the mean square displacement at moderation) proved to be equal to L^2_f (1.46 ev) = 92 ± 1.5cm^2, L^2_f (0.3 ev) = 104.5±2.0cm^2. Their difference L^2_f(1.46 → 0.3ev) = 12.5±2.5 cm^2 exceeds the value calculated by 60% with the assumption that a neutron collides with free atoms. Thus, in the range 1.46–0.3 ev the atom bond in BeO lattice significantly effects on the neutron moderation. The value of L^2_f(1.46 ev) is in agreement with the data obtained [11,12] but it is more accurate. There are no data available for L^2_f (0.3) in literature.

4. Study of Neutron Slowing-Down in Be and BeO

The slowing-down of neutrons ~ 2 Mev in Be and BeO was studied on the linear accelerator of the IAE by impulse method, measuring the transmission for indium, cadmium and samarium filters (In, Cd, Sm have strong resonances at 1.46 ev, 0.178 ev and 0.0976 ev, respectively) by a small BF_3-counter. In addition to BF_3-counter the detector of 0.3 ev neutrons was also used. The detectors were placed in moderator block (Be–60^{3}cm^3, BeO–70.80.75 cm^3) along the neutron beam axis of the accelerator.

The measurement results for the value of the inverse transmission $\Pi^{-1}(t)$ vs time, which lasted after a neutron impulse moment, are shown in Fig. 10. In the same figure the detector counting rate of 0.3 ev neutrons is given too (Pu-chamber, shielded by Sm+Cd). In these measurements the channel width of the time analyzer was from 1μ sec to 10μ sec.

From the curves of Fig.10 the maxima are clearly seen. For convenience, $\Pi^{-1}(t)$ is normalized to unit. The time corresponding to these maxima is obviously a neutron slowing-down time up to a given energy, t_s , plus the time of flight from the point of the last collision up to the neutron absorption in detector $t_f\left(\lambda_s(v) + \frac{d}{2}\right)/v$ where v is the neutron velocity, d is the mean detector dimension (taking into account the detector hole).

In Table III the values t_s are given. The errors result from the uncertainty of the position of the maximum, the former is connected with the channel analyzer width and with the inaccuracy of the calculation of t_f . The comparison of these values with calculated ones, obtained for the neutron scattering by free atoms shows that the crystical binding in Be and BeO is of importance for the slowing-down already in 1.46–0.3 ev range.

Measuring with Pu-chamber (Fig.14) made possible to derive another important slowing-down characteristic-time-energy distribution of moderating neutrons of 0.3 ev and to compare it with the theoretical one [13]:

$$N(\tau, u, t) \frac{\xi v}{\lambda_s} N_{cm}(\tau, u) N_o(u, t)\left[1+\varepsilon(\tau, u, t)\right], \quad (3)$$

where

$$N_o(u,t) = \frac{\left(1-\frac{v}{v_o}\right)^{2/\xi - 1}}{\xi} \frac{\left(\frac{vt}{\lambda_s}\right)^{2/\xi}}{\Gamma\left(1+\frac{2}{\xi}\right)} e^{-\frac{vt}{\lambda_s}}, \quad (4)$$

$N_o(u,t)$ is Poisson probability of appearence of $2/\xi$ neutrons during a time t, if the neutron appearence at any moment is equally probable and equal to $\frac{v}{\lambda_s} dt$ (u is lethargy, v_o and v are initial and final neutron velocities). The full and dotted lines in Fig.11 correspond to Poisson distribution (4) with $2/\xi$ = 12 for Be and 18 for BeO, respectively. The discrepancy of theory and experiment at large t is connected with the effect of slowly increasing factor $1+\varepsilon$ in formula (3).

From the fact that the dispersion of Poisson distribution equals the average value and using the relations $\left(\frac{v t_s}{\lambda_s}\right)_{Be} = \frac{2}{\xi_{Be}} = 12$ and $\left(\frac{v t_s}{\lambda_s}\right)_{BeO} = 2/\xi_{BeO} = 18$, the slowing down time t_s up to the energy 0.3 ev can be obtained independently of its determination from the position of the maximum (see Table III). For this purpose the dispersion $\Delta t = \frac{\Delta v}{v} t_s = \frac{1}{2} \frac{\Delta E}{E} t_s$ (2.9μ sec for Be and 4.5μ sec for BeO) which is connected with energy range of detector sensitivity [10] , is to be substracted from t_s. As a result we get 17.3μ sec for Be and 28μ sec for BeO, and also ξ_{Be} = 0.19 and ξ_{BeO}=0.12.

The neutron slowing-down below 0.1 ev was studied by the measurement of the transmission

of boron filters of 0.012 g/cm^2 and 0,023 g/cm^2 with I/V-detector, the detectors and filters being placed outside the block (see Fig.12). Due to collimator I only those neutrons may be detected which were directed to a block surface at the angle > 80°. It simplified significantly the calculation of the filter transmission $\Pi(T)$ vs the neutron temperature T. It was used then for deriving the temperature of moderated neutrons at the moment t from the transmission values measured with the assumption of Maxwellian distribution (see Figs.13 and 14, where T_φ is the equilibrium temperature at $t \to \infty$). In the calculations of $\Pi(T)$ either theoretical results for $\sigma_{tr}(E)$ in Be and BeO [14] were used or the experimental data obtained in [15] for σ_t in Be and our data for σ_t in BeO with the grain size 8μ. The full and dotted lines in Fig.15 a,b correspond to these two ways of calculation of $\Pi(T)$. It is seen from these figures that below 0.7-0.5 ev T(t) tends to T_φ exponentially, the relaxation time γ^{-1} being practically independent of neither the filter thickness nor the way of calculation $\Pi(T)$. Besides the data in Fig. 13 and 14 the values γ^{-1} for beryllium blocks of 50^3 cm^3 and for beryllia blocks of 60^{3}cm^3 were measured. After correcting for finite block sizes, the thermalization time $t_{th} = 185 \pm 20\mu$ sec for Be and $t_{th} = 204 \pm 20\mu$ sec for BeO, as a result, was obtained.

The measurements of t_s and t_{th} performed, give the possibility for deriving the value ξ and making the following conclusions. The neutron slowing-down to 1.46 ev in Be and BeO is due to collisions with free atoms and lasts less than 10μ sec. In the range 1.46-0.3 ev a crystal binding effect reduced ξ to 0.193$\pm$0.02 in Be and to 0.109$\pm$0.012 in BeO; t_s in this range is 1.5-2 more than t_s to 1.46 ev. In the range 0.3 $\sim$ 0.5 ev, below which the spectrum approximating that of Maxwellian is established, $\xi_{Be} = 0.049 \pm 0.005$ and $\xi_{BeO} = 0.047 \pm 0.005$ and t_s is 6-7 more than t_s to 1.46 ev. At E $\lesssim$ (0.05-0.025 ev) the moderation is very slow, on an average, up to 185μ sec ξ in Be and up to 204μ sec in BeO. The mean logarithmic energy loss in this range for the whole neutron spectrum is dependent on the energy and determined by the thermalization time:

$$\bar{\xi} = \frac{\lambda_s}{t_{th} v_\varphi} \sqrt{\frac{E_\varphi}{E}} \frac{E - E_\varphi}{E}$$

where E_φ and v_φ are the equilibrium energy and velocity.

The energy-time distribution of neutrons in the range to $\sim$ E $\simeq$ 0.05 ev can be obtained from formula (4) by substituting the given values ξ. The same values were used for calculation of the slowing-down area below 1.46 ev (see Table IV).

The value L^2_f (0.3 ev) for BeO is in a good agreement with the direct measurement data (see § 3).

5. Multiplication of Fission Neutrons in Be and BeO in Be^9 (n, 2n) Reaction

The moderators containing Be give an additional neutron multiplication in reactors connected with the difference of contributions of (n,2n) and (n, α) reactions. As the calculation of the coefficient of this multiplication possessed a large uncertainity [17], we measured K_{Be} for Be in spherical geometry experiment. The experiment consisted in measurement of integral neutron fission source power N (fission converter of U^{235} on the reactor beam), being shielded by a spherical layer of beryllium or graphite of various thickness (graphite was necessary for excluding the variation of the sensitivity of the detector ("allwave" BF_3-counter) with neutron energy). The presence of a hole in a beryllium and graphite spheres for transmission of reactor neutron beam into converter caused the anisotropy of fission source and led to determining the source power N as a result of integrating the counting rate, measuring on a horisontal plane at different angles to the beam axis. For reducing this anisotropy and excluding the corrections for a finite distance from the source to the detector, the spheres investigated were surrounded by a spherical wood layer 14 cm thick.

In Fig.16 the measurement results are shown of N_0 and N_{Be} vs the mean neutron energy loss $\Delta\bar{E}$ when neutrons passed the graphite and beryllium layers and also $K_{Be} = N_{Be}(\Delta\bar{E})/N_0(4\bar{E})$ is

362 a

given. The value $\Delta\bar{E}$ was calculated with the effect of neutron "entangling" in elastic and inelastic collisions with Be and C, and it contains some uncertainity which is however of no importance for K_{Be} (see Fig.17). Curve 2 of Fig.17 gives the more probable run of Σ_{Be} vs a layer thickness. At 12–15 g/cm^2 Be K_{Be} obtains the maximum value 1.10±0.015. Using this value, the multiplication coefficient of fission neutrons was calculated in BeO too. It was assumed that $\frac{K_{BeO}-1}{K_{Be}-1} = \frac{n_{BeO}}{n_{Be}}$ where n_{Be} and n_{BeO} are the fission neutron collision density with beryllium atoms at neutron slowing-down in Be and BeO below the threshold of $Be^9(n, 2n)$, $Be^9(n, \alpha)$ and $O^{16}(n,\alpha)$ reactions. This assumption is approximately true, as at E > 4 Mev $\sigma_{n,2n}$ is nearly constant, and at E < 4 Mev the collision densities in Be and BeO are similar. As a result, $\frac{n_{BeO}}{n_{Be}} = \frac{1.34}{1.62}$ was obtained. Hence $K_{BeO} = 1.08\pm0.023$.

B. CONTRIBUTION OF FAST EFFECTS ON Be TO THE MULTIPLICATION COEFFISIENT OF BERYLLIUM ASSEMBLIES

A.K.Krasin, G.I.Plindov,
The Institute of Energetics of Academy of Sciences
USSR

It is of interest to take into account the effect of (n,2n) and (n,α) reactions on Be on critical masses and sizes of physical beryllium assemblies and to separate the contribution of fast effect into the multiplication coefficient.

For this purpose 10-group constants for beryllium were obtained. The Be (n,2n) reaction has considered as inelastic scattering leading to an additional neutron. The cross-sections of (n,2n) and (n,α) reactions were taken in from [18–22] and [23,25], respectively.

For verification of constants obtained the neutron age of fission spectrum and fast-neutron multiplication coefficient in infinite homogeneous beryllium medium were calculated. The evaluated neutron age τ = 79 cm^2 and the value of fast neutron multiplication coefficient K_{Be} = 1.087 were obtained, which are in a good agreement with the data [26] and with theoretical estimations [27,28], respectively.

With these constants the multiplication coefficients, critical masses and critical dimensions of physical assemblies, described in [29], were calculated in multi-group diffusion approximation, taking into account the reactions Be (n,2n) and Be (n,α) ("a"-case) and with no account of them ("b"-case). The contribution of the fast effect on Be was defined as a difference of the multiplication coefficients, calculated with the account of Be(n,2n) and Be (n,α) reactions or without it.

The results of calculations are shown in Table V. It is seen from Table V that the value of the fast effect on 9–10% Be is somewhat less, than the value 12±4% given earlier for the same assemblies [29], but is within the experimental errors. Since the fast effect on Be was calculated in multigroup theory, the value of the present work seems more preferable.

3629

ЛИТЕРАТУРА

1. И.Ф. Жежерун, И.П.Садиков, А.А.Чернышов, Атомная энергия 13, 250 (1962); И.Ф.Жежерун, И.П.Садиков, В.А.Тарабанько, А.А.Чернышов. Атомная энергия 13, 258 (1962); И.Ф.Жежерун. Атомная энергия 14, 193 (1963); И.Ф.Жежерун, И.П.Садиков, В.А.Тарабанько, А.А.Чернышов. Атомная энергия 15, 485 (1963); И.Ф.Жежерун. Атомная энергия 15, 505 (1963); И.Ф.Жежерун. Атомная энергия 16, 234 (1964); И.Ф.Жежерун. Изучение процесса замедления нейтронов в бериллии и окиси бериллия импульсным методом. Не опубликовано. Основные результаты докладывались на Женевской конференции.
2. А.В.Антонов и др. В книге "Физические исследования" Москва, изд-во АН СССР, 1955, стр.158 (Доклады советск.делегации на международной конференции по мирному использованию атомной энергии. Женева, 1955).
3. E.Campbel, P.Stelson. ORNL, 2076 (1956).
4. T.Komoto, F.Kloverstrom. Trans.Amer.Nucl.Soc., 1, 94 (1958).
5. G.de Saussure and E.G.Silver. Nucl.Sci.Abstr., 13, 1059 (1959); Nucl.Sci.and Eng.,6, 195 (1959); Proc. of Symposium Vienna, 17-20 October, 1960, p.500.
6. S.D.B.Iyenger, G.S.Mani, R.Ramanna and N.Umakanth Proc.Ind.Acad.Sci., XLV, s A, 265 (1957).
7. L.S.Kothary, P.G.Khubchandany, React. Sci.and Technol., 15, 30 (1961).
8. K.W.Seeman, Nucl. Sci.Abstr., 15, 1407 (1962).
9. G. de Saussure. Nucl.Sci. and Eng., 12, 433 (1962).
10. И.Ф.Жежерун, И.П.Садиков, А.А.Чернышов "Приборы и техника эксперимента" № 3, 43 (1962).
11. P.Benoist et al. Доклад № II92, представленный Францией на вторую международную конференцию по мирному использованию атомной энергии (Женева, 1958).
12. G.A.Joanon, A.J.Goodjohn and N.F.Winker. Nucl.Sci.and Eng., 13, 171 (1962).
13. И.Г.Лядькин, Б.Н.Ботолина, Атомная энергия, 10, 5 (1961).
14. К.Сингви, Л.Кохари. Труды второй международной конференции по мирному использованию атомной энергии. Женева, 1958 г. Избранные доклады иностранных ученых, т.2, стр.675. Атомиздат, Москва, 1959.
15. Д.Х.Хьюдж, Р.Б.Шварц. Атлас нейтронных сечений. Издание второе. Атомиздат, Москва, 1959.
16. Д.Юз. Нейтронные исследования на ядерных котлах, стр.161. Изд.иностранной литературы, Москва, 1954.
17. H.Kief, Nucl. Sci.and Eng., 10, 83 (1961).
18. J.S.Marion, J.S.Levin and L.Cranberg Phys.Rev., 114,(1959) p.1584.
19. G.J.Fischer,Phys. Rev. 108, 99 (1957).
20. J.R.Beyster, R.L.Henkel, R.A.Nobles and J.M.Kister. Phys.Rev., 98, 1216 (1955).
21. Ю.Г.Зубов, Н.С.Лосседев, В.М.Мороз. Сборник "Нейтронная физика" Госатомиздат, М.,1961.
22. W.F.Ball, M. McGregov and R.Booth, Phys.Rev., 110, 1392 (1958).
23. P.H.Stelson and E.C.Campbell, Phys.Rev., 106, 1252 (1957).
24. M.E.Battat and F.L.Ribe. 89, 80 (1953).
25. R.Base and T.W.Bonner. Nucl.Phys.,23, 122 (1961).
26. М.Шапиро. Материалы комиссии по атомной энергии США. Ядерные реакторы, т.I,М.,(1956) 206.
27. K.C.Xines and J.R.Pollard, Journ.of Nucl.Energy, Part A-B, 16, 7 (1962)
28. P.G.Aline, P.E.Novak and B.Wolfe. Nucl.Sci.and Eng., 7, № 4, Letters (1960).
29. А.К.Красин, Б.Г.Дубовский, М.Н.Лонцов, Ю.Ю.Глазков, Р.К.Гончаров, А.В.Кашаев, Л.А.Ре[illegible]ва, В.В.Вавилов, Е.И.Инютин, А.П.Сенченков. Труды Международной конференции по использованию атомной энергии в мирных целях.II Женева (1958). Доклад № 2146.

362а

Table 1

Value of $\bar{\sigma}_t$ and $(\bar{\sigma}_t^{-1})^{-1}$ averaged over the Maxwellian spectrum at the neutron temperature T_n = 390°K

Sample	Grain sizes, μ		$\bar{\sigma}_t$, barn	$(\bar{\sigma}_t^{-1})^{-1}$, barn
	advantageous	average		
I	10–15	8	9.97	9.13
2	40	29	9.44	8.31
3	10–20	13	9.56	8.53
4	–	14	9.70	8.76

Table II

Diffusion parameters of Be and BeO

Parameters	units	In Be	In BeO
$\varepsilon_c v$	sec^{-1}	262 ± 11	174 ± 6
D	cm^2/sec	$(1.24 \pm 0.013) \cdot 10^5$	$(1.56 \pm 0.01) \cdot 10^5$
C	cm^4/sec	$(3.68 \pm 0.20) \cdot 10^5$	$(4.12 \pm 0.27) \cdot 10^5$
L	cm	21.8 ± 1.0	29.9 ± 1.0
Transfer length, λ_{tr}	cm	1.50 ± 0.016	1.88 ± 0.020
Diffusion time, e	msec	3.82 ± 0.017	5.75 ± 0.020
Absorption cross section σ_c at 2200 m/sec	mbarn	10.0 ± 0.4	11.8 ± 0.4

Table III

Slowing-down time (in μ sec) of ~ 2 Mev neutrons to various energies

Slowing-down energy, eV	In Be		In BeO	
	calculation ξ = 0.209	experiment	calculation ξ = 0.176	experiment
1.46 (In)	7.2	7.5 ± 1	9.3	9.5 ± 1
0.3 (Pu)	15.7	17.5 ± 1	19.2	26 ± 2
0.178 (Cd)	20.4	40 ± 3	26.3	51 ± 3
0.0976 (Sm)	27.6	73 ± 5	34.8	88 ± 5

362a

Table IV

Slowing-down time τ_s and area L_s^2 of neutrons up to 1.46 ev in Be and BeO

Energy range	In Be		In BeO	
	τ_s, μ sec	L_s^2, cm^2	τ_s, μ sec	L_s^2, cm^2
2 MeV – 1.46 eV	7.5±1	85.8±16	9.5±1	92±1.5
2 MeV – 0.3 eV	17.5±1	91.5±2.4	27±2	103.4±1.9
2 MeV – 0.178 eV	40±3	98.9±26	51±3	112.1±2.1
2 MeV – 0.13 eV	56±4*)	103.4±2.7	69±4*)	117.7±2.4
2 MeV – 0.0976 eV	73±5	107.5±2.9	83±5	122.5±2.9
2 MeV – (0.07–0.045)eV	135	-	160	-
(0.07–0.045) – 0.025 eV	185±20	-	204±25	-

*) It is calculated using the obtained values of τ in the energy range 0.3 – 0.0976 ev.

Table V

Calculation results of K_{eff}, critical sizes, critical masses and fast effect on Be

Assembly		K_{eff}	R_{cal} cm	R_{exp} cm	M_{cal} kg	M_{exp} kg	K_{Be}
graphite in fuel element	4a	1.0301	37.9	40.4	4.8	5.46	0.1016
	4b	0.9286	48.4				
	5a	1.0341	34.7	37.5	5.02	5.86	0.0997
	5b	0.9344	44.6				
	6a	1.0241	34.3	36.5	6.10	6.66	0.0971
	6b	0.9270	45.3				
water in fuel element	4a	1.0396	28.9	31.5	2.78	3.31	0.0949
	4b	0.9447	36.5				
	5a	1.0431	25.8	28.4	2.79	3.36	0.0928
	5b	0.9503	32.5				
	6a	1.0420	23.9	26.2	2.85	3.42	0.0912
	6b	0.9508	30.0				

362a

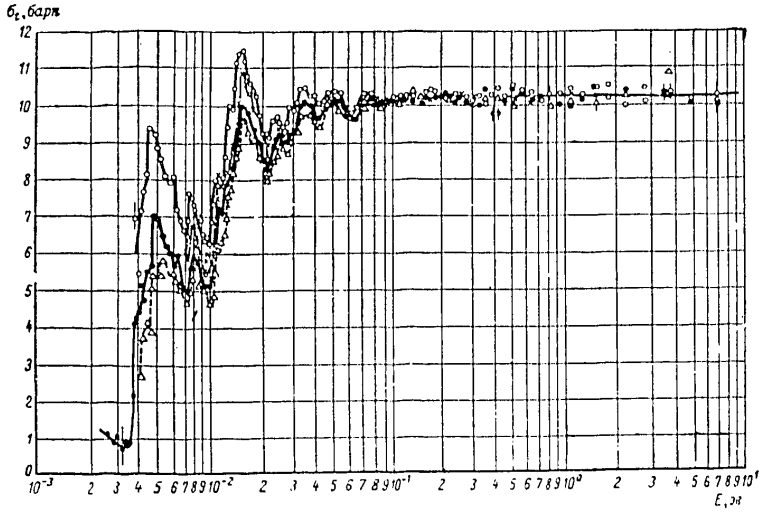

Fig.1. Total cross section σ_t for the BeO samples of various crystal grain sizes; sample 1 (○): grain sizes = 4–23 μ, average size = 8 μ, advantageous sizes = 10–15 μ; 2 (▽): sizes = 9–60 μ, average one = 29 μ, advantageous one = 40 μ; 3 (•): sizes = 5–37 μ, average one = 13 μ, advantageous ones = 10–20 μ; 4 (x): sizes are large than ones of I and are less than ones of 3, average size = 14 μ.

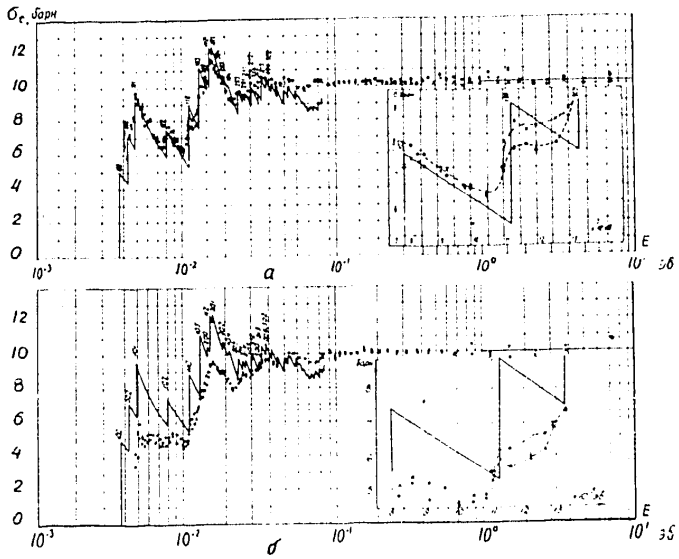

Fig.2. Total cross section for samples I and 2 produced by extrusion (a) and pressing (b). The incident neutron beam is parallel (•) and is normal to direction of extrusion and of pressing (x). The partial cross sections for the reflection from the plane (110) (see the insert) differ by 20–25%. The solid line represents the value of σ_s calculated with the assumption or absence of the extinction and the account of only elastic scattering.

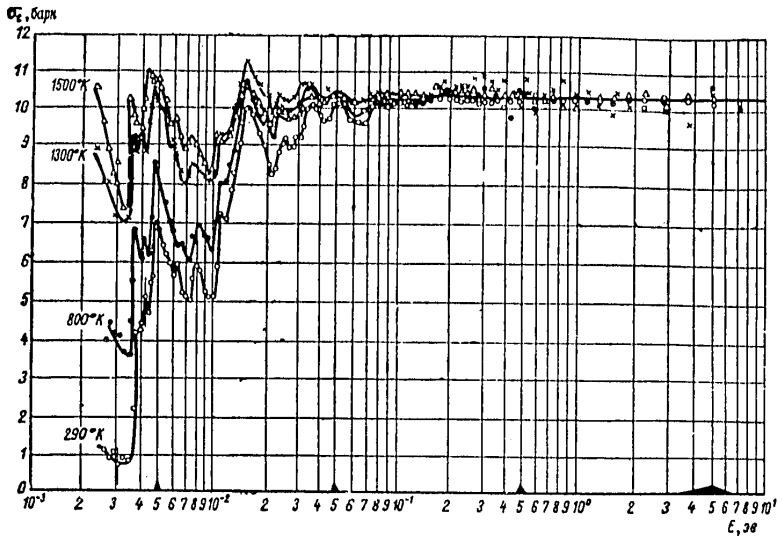

Fig.3. Total cross section σ_t for BeO at various temperatures

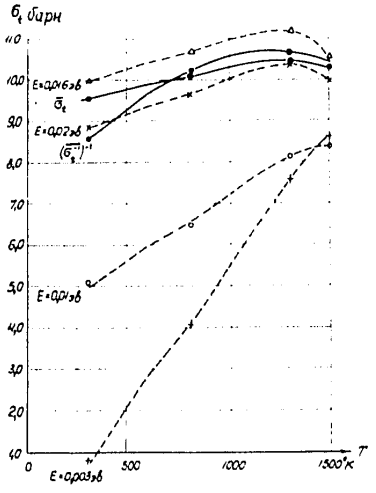

Fig.4. Total cross section for BeO vs temperature. $\bar{\sigma}_t$ and $(\bar{\sigma}_t^{-1})^{-1}$ are averaged over the Maxwellian spectrum for neutron temperature $T_n = T + 100°K$.

362 a

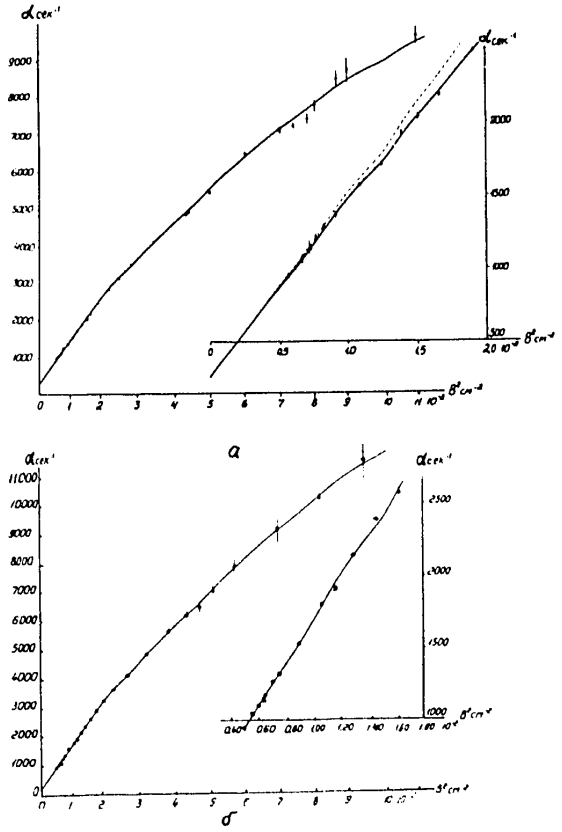

Fig.5. Damping coefficient α vs B^2 for Be (a) and BeO(b). The dots are the measurement results, the solid line corresponds to parabola (see Eq.(1) and Table II).

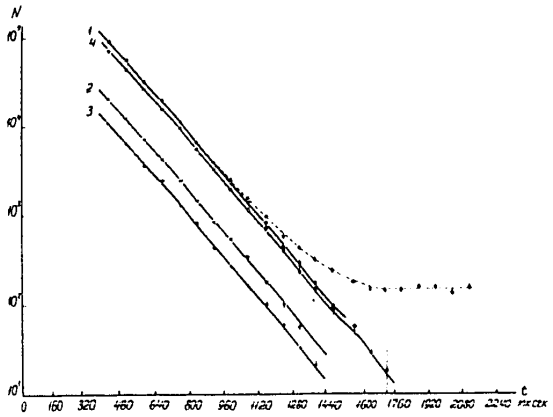

Fig.6. Neutron density damping in Be block of $20^3 cm^3$. 1,2,3 are various powers of a neutron source; 4-with the large background level. The dotted line represents the background plus the effect, the solid lines are obtained after the substraction of the background.

362 a

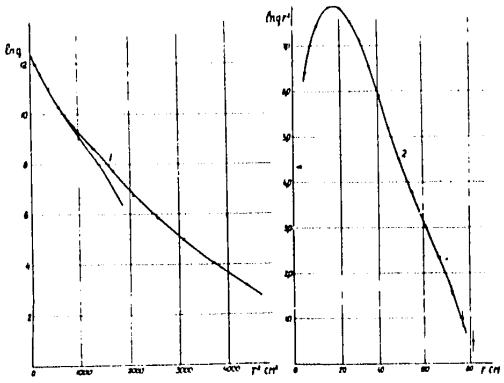

Fig.7. Moderation density at E = 1.46 eV for BeO in various coordinates

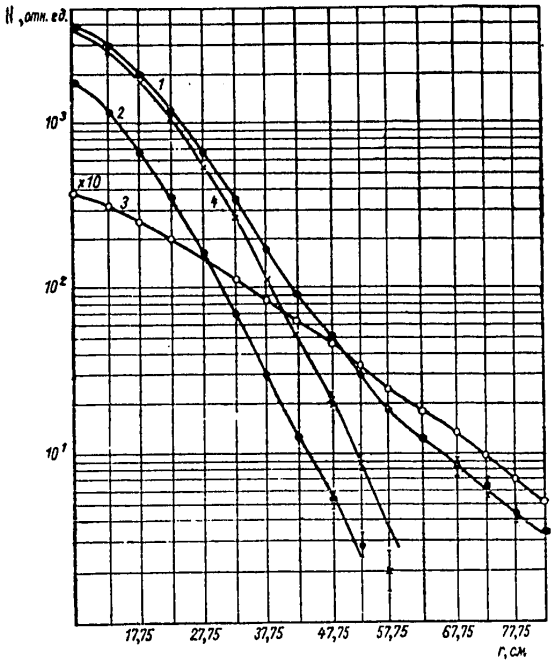

Fig.8. Measurement results with Pu-chamber: (1) flux of 0.3 ev neutrons $\Phi_{0.3}$ (2) contribution of higher resonances; (3) thermal neutron flux Φ_T; (4) moderation density q at E = 0.3 ev. I - relative unit, II-g, cm

362a

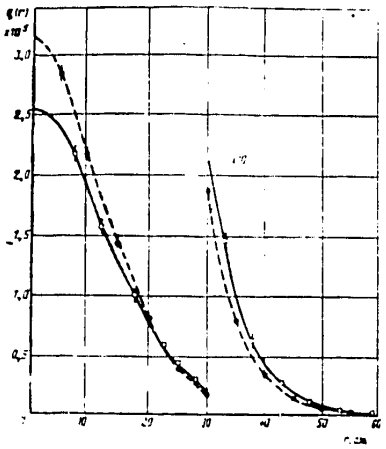

Fig.9. Comparison of the slowing-down densities at 0.3 ev(o) and 1.46 ev(•). The solid and dotted lines correspond the synthetic nuclei of type (2) at E_r=0.3 ev and 1.46 ev.

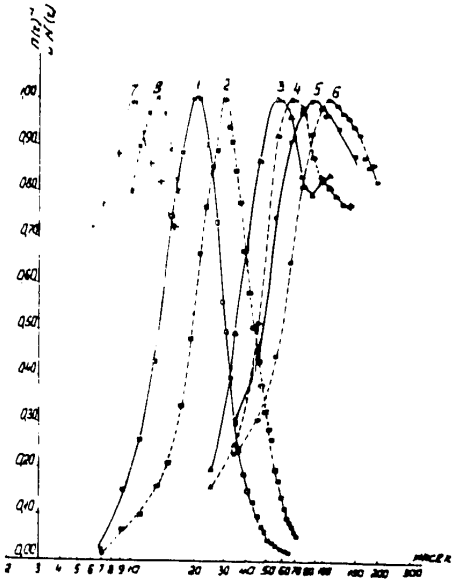

Fig.10. Measurement results of the slowing-down time. 1,2 are the detector counting rates N(t) of 0.3ev neutrons in blocks of Be and BeO, respectively; the inverse transmission $n^{-1}(=)$ of Cd(3,4), Sm (5,6) and In(7,8) filters in Be and BeO.

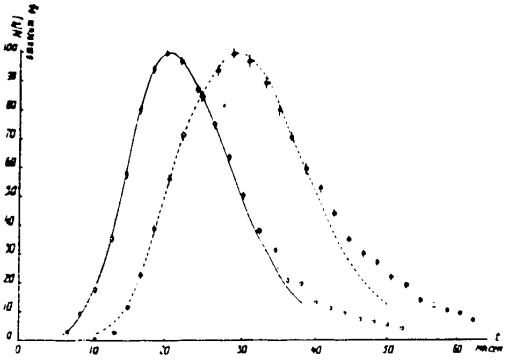

Fig.11. Experimental energy-time distribution of slowing-down neutrons at E =0.3 ev in comparison with the theoretical one. ○● -experiment for Be and BeO. The solid and dotted lines correspond to Poisson distribution: $N_{Be} \sim \left(\frac{vt}{\lambda_s}\right)^{12} e^{-\frac{vt}{\lambda_s}}$,

$$N_{BeO} \sim \left(\frac{vt}{\lambda_s}\right)^{18} e^{-vt/\lambda_s}$$

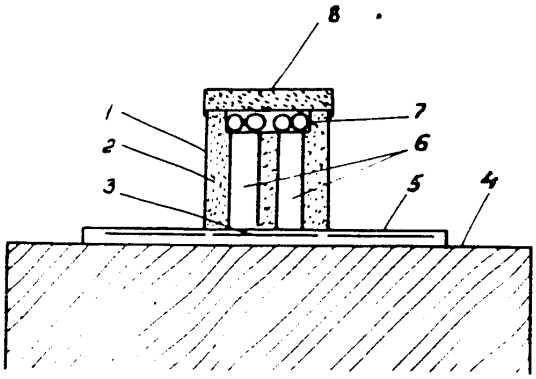

Fig.12. Experimental arrangement for studying of transmission through boron. 1-neutron collimator with Cd and ByC; 2,3-filters; 4-moderator block; 5-collimator support; 6-collimator holes; 7-BF_3-counter; 8-shield of counters.

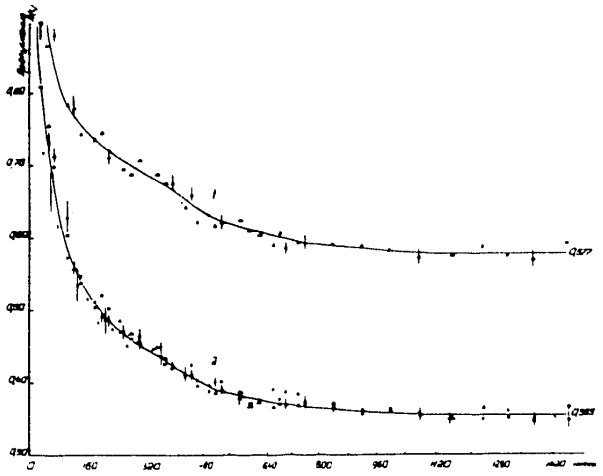

Fig.13. Transmission of boron filters for the Be block 60³cm³; I-filter 0.012 g/cm²; 2-filter 0.023 g/cm²; ○●×▲ -various measurement series.

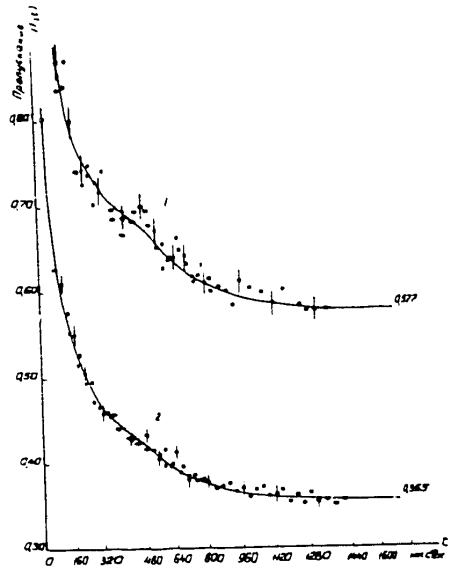

Fig.14.Transmission of boron filters for BeO block 70x80x75 cm³. I-transmission; II-μ sec.

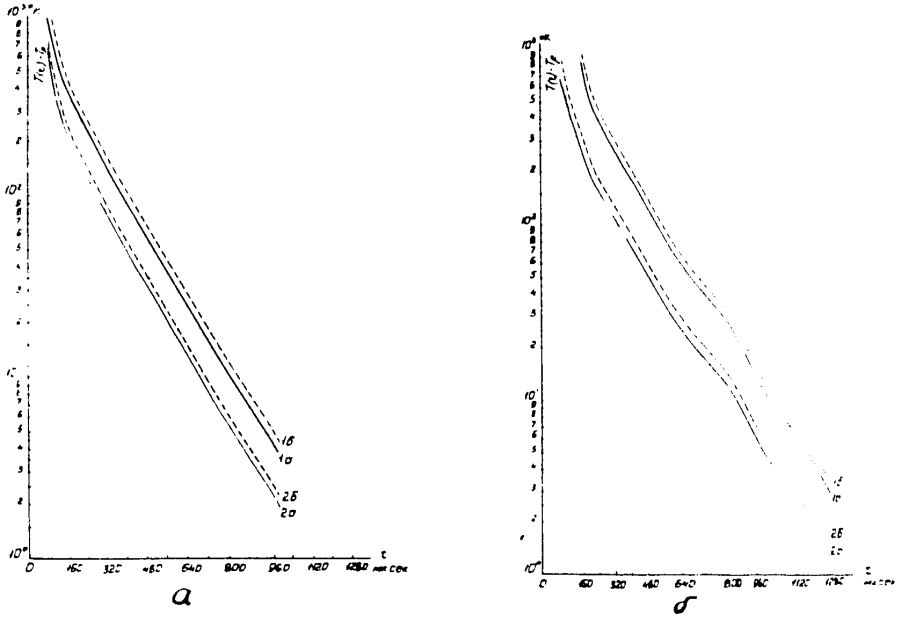

Fig.15. Neutron temperatures in Be(a) and BeO(b) vs slowing-down time (obtained from plats of Fig.13 and 14).

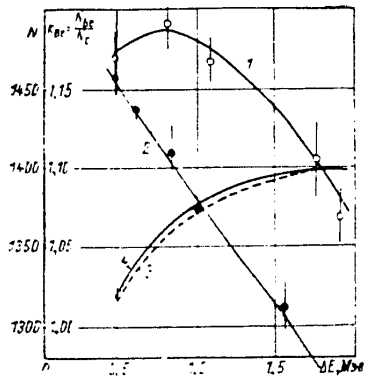

Fig.16. Integral counting rate N vs the average neutron energy loss $\Delta\bar{E}$: 1 - Be layer; 2 - graphite layer; 3 - $K_{Be}=N_{Be}(\Delta\bar{E})/N_c(\Delta\bar{E})$; 4 - K_{Be} with correction of hole effect in spheres for the transmission of neutron beam

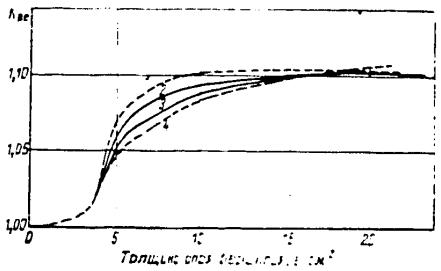

Fig.17. Effect of $\Delta\bar{E}$ calculation inaccuracy upon K_{Be}. The calculation variants: 1-with utilization of cross-sections on 15% as large in comparison with the data [15]; 2 - with utilization of cross-sections [15]; 3 - K_{Be} with the account of neutron absorption in a wood sphere; 4 - with an assumption that $\sigma_{s_1}=\sigma_{s_2}$. 1 - Beryllium layer thickness, g/cm^2